

Doppler Sonography in Infancy and Childhood

Karl-Heinz Deeg
Thomas Rupprecht
Michael Hofbeck

 Springer

Doppler Sonography in Infancy and Childhood

Karl-Heinz Deeg • Thomas Rupprecht
Michael Hofbeck

Doppler Sonography in Infancy and Childhood

With contributions by
Doris Franke
Michael Riccabona
Heiko Dudwiesus

 Springer

Karl-Heinz Deeg
Klinikum Bamberg Kinderklinik
Bamberg
Germany

Michael Hofbeck
Universitätskinderklinik Tübingen
Abt Kinderkardiologie
Tübingen
Germany

Thomas Rupprecht
Klinikum Bayreuth GmbH Klinik für
Kinderheilkunde/Jugendmedizin
Bayreuth
Germany

ISBN 978-3-319-03505-5 ISBN 978-3-319-03506-2 (eBook)
DOI 10.1007/978-3-319-03506-2
Springer Cham Heidelberg New York Dordrecht London

Library of Congress Control Number: 2014936294

© Springer International Publishing Switzerland 2015

This work is subject to copyright. All rights are reserved by the Publisher, whether the whole or part of the material is concerned, specifically the rights of translation, reprinting, reuse of illustrations, recitation, broadcasting, reproduction on microfilms or in any other physical way, and transmission or information storage and retrieval, electronic adaptation, computer software, or by similar or dissimilar methodology now known or hereafter developed. Exempted from this legal reservation are brief excerpts in connection with reviews or scholarly analysis or material supplied specifically for the purpose of being entered and executed on a computer system, for exclusive use by the purchaser of the work. Duplication of this publication or parts thereof is permitted only under the provisions of the Copyright Law of the Publisher's location, in its current version, and permission for use must always be obtained from Springer. Permissions for use may be obtained through RightsLink at the Copyright Clearance Center. Violations are liable to prosecution under the respective Copyright Law.

The use of general descriptive names, registered names, trademarks, service marks, etc. in this publication does not imply, even in the absence of a specific statement, that such names are exempt from the relevant protective laws and regulations and therefore free for general use.

While the advice and information in this book are believed to be true and accurate at the date of publication, neither the authors nor the editors nor the publisher can accept any legal responsibility for any errors or omissions that may be made. The publisher makes no warranty, express or implied, with respect to the material contained herein.

Printed on acid-free paper

Springer is part of Springer Science+Business Media (www.springer.com)

Contents

1	Physical and Technical Principles of Doppler Sonography . . .	1
1.1	Doppler Effect.	2
1.1.1	Summary.	4
1.2	Continuous Wave Doppler Ultrasound Technique	7
1.3	Spectral Analysis	9
1.4	Angle Problem	11
1.5	Pulsed Doppler Devices	14
1.6	Duplex Systems	19
1.7	Colour-Coded Doppler Sonography	20
1.8	Triplex Mode.	26
1.9	Setting the Colour Threshold	27
1.10	Movement Disturbances and Wall Filters.	28
1.11	Adjusting the Gain	30
1.12	Power Doppler	30
1.13	3D Dopplers	31
1.14	Non-Doppler-Based Flow Recording	32
	References	34
2	Cerebral Doppler Sonography	37
2.1	Introduction.	38
2.2	Normal Anatomy of the Cerebral Arteries	39
2.2.1	Sagittal Sections	39
2.2.2	Parasagittal Sections.	42
2.2.3	Coronal Sections.	44
2.2.4	Axial Sections.	48
2.2.5	Flow Measurements	54
2.2.6	Normal Flow Velocities in the Intracranial Arteries in Healthy Infants	55
2.3	Normal Anatomy of the Cerebral Veins	64
2.3.1	Sagittal Sections	64
2.3.2	Coronal Sections.	66
2.3.3	Axial Sections.	73
2.3.4	Flow Measurements and Normal Values	73

2.4	Intracranial Haemorrhage	78
2.4.1	Intracranial Haemorrhage of Preterm Infants . .	78
2.4.2	Subdural and Epidural Haemorrhage	89
2.4.3	Subarachnoid Haemorrhage	96
2.5	Pericerebral Fluid Collection	96
2.6	Hydrocephalus	103
2.7	Meningoencephalitis	116
2.7.1	Postnatal Meningoencephalitis	116
2.7.2	Prenatal Infections of the Brain	122
2.8	Hypoxaemic-Ischaemic Encephalopathy	127
2.8.1	Hypoxic-Ischaemic Lesions in Preterm Babies .	127
2.8.2	Hypoxic-Ischaemic Injury in Term-Born Babies	128
2.9	Doppler Sonographic Diagnosis of Stroke in Infants	139
2.9.1	Ischaemic Occlusion (Arterial Infarct)	142
2.9.2	Haemorrhagic Stroke (Cerebral Venous Thrombosis)	147
2.10	Vascular Malformations	154
2.10.1	Arteriovenous Malformation (AVM) of the Vein of Galen	154
2.10.2	Other Intracranial Vascular Malformations and Vascular Diseases	164
2.11	Doppler Sonography in Cerebral Tumours and Other Space-Occupying Lesions	165
2.11.1	Arachnoid Cysts	165
2.11.2	Intracranial Tumours	166
2.12	Flow Measurements in the Basilar Artery of Infants at Risk to Die of Sudden Infant Death	169
2.13	Doppler Sonographic Characteristics of Brain Death	181
2.14	Influence of Various Procedures on the Flow Velocities in Intracranial Vessels	183
2.14.1	Effect of Phototherapy on Cerebral Blood Flow	183
2.14.2	Effect of a Painful Stimulus on Cerebral Blood Flow	183
2.14.3	Effect of Ketamine on Neonatal Cerebral Circulation	183
2.14.4	Effect of Fentanyl on Cerebral Haemodynamic in Sick Newborn Infants	184
2.14.5	Effect of Seizures and Generalised Epileptic Discharge on Intracranial Blood Flow Velocities	184
2.14.6	Influence of Antiepileptic Therapy on Cerebral Haemodynamics	184
2.14.7	Effect of Theophylline and Aminophylline Therapy on Cerebral Circulation	184

2.14.8	Effect of Caffeine Therapy on Cerebral Circulation	185
2.14.9	Effect of Indomethacin Therapy on Cerebral Circulation	185
2.14.10	Effect of Ibuprofen Treatment on Cerebral Circulation.	186
2.14.11	Effect of Surfactant Treatment on Cerebral Circulation	186
2.14.12	Effect of Dexamethasone and Hydrocortison Treatment on Cerebral Circulation	187
2.14.13	Effect of Doxapram Therapy on Cerebral Circulation	187
2.14.14	Influence of Umbilical Artery Catheter Blood Sampling on Cerebral Circulation	188
2.14.15	Influence of the Mode of Ventilation on Cerebral Perfusion.	188
2.14.16	Influence of Inhaled Nitric Oxide on Cerebral Blood Flow Velocity.	188
2.14.17	Influence of Anaemia on Cerebral Blood Flow.	188
2.14.18	Influence of Anaesthesiologic Medication on Neonatal Cerebral Circulation.	188
	References	189
3	Transcranial Colour Doppler Sonography (TCDI)	195
3.1	Introduction to TCDI.	196
3.1.1	Vascular Supply of the Brain	196
3.1.2	Investigation Technique and Normal Findings	196
3.1.3	Intracranial Venous Anatomy	202
3.1.4	Contrast Agents and Perfusion Imaging	202
3.1.5	Interpretation of Transcranial (Colour) Doppler Imaging	204
3.2	Clinical Indications of Transcranial Colour Doppler Imaging (TCDI).	209
3.2.1	Diagnosis of Intracranial Vascular Disease (Arteritis, Occlusion, Stenosis).	209
3.2.2	General Considerations.	210
3.2.3	Brain Oedema	212
3.2.4	Detection of Arteriovenous Malformations (AVMs).	218
3.2.5	Investigations in Childhood Migraine.	220
3.3	Brain Death	222
3.3.1	Pitfalls (Haemodynamic Effects of Extracranial Disease and Influences of Physiological States on the Intracranial Blood Flow Velocities).	222
	References	226

4 Doppler Sonography of the Head and Neck	229
4.1 Method	230
4.2 Pathologic Indications	232
4.2.1 Diseases of the Thyroid Gland	232
4.2.2 Cervical Lymphadenopathy	242
4.2.3 Fibromatosis Colli	250
4.2.4 Cystic Masses	255
4.2.5 Vascular Tumours	259
4.2.6 Miscellaneous	264
References	271
5 Doppler Sonography of the Abdominal Vessels	273
5.1 Abdominal Arteries	274
5.1.1 Abdominal Aorta	274
5.1.2 Coeliac Artery	276
5.1.3 Hepatic Artery	279
5.1.4 Splenic Artery	281
5.1.5 Left Gastric Artery	282
5.1.6 Superior Mesenteric Artery (SMA)	282
5.1.7 Renal Arteries	285
5.2 Abdominal Veins	288
5.2.1 Inferior Vena Cava	288
5.2.2 Portal Venous System	289
5.2.3 Hepatic Veins	295
5.2.4 Physiologic Remnants of the Foetal Circulation: Ductus Venosus Arantii	297
5.2.5 Renal Veins	297
5.3 Thrombosis of the Abdominal Aorta and Vena Cava Inferior	300
5.4 Displacement of the Abdominal Aorta and Inferior Vena Cava by Space-Occupying Lesions	300
5.5 Coeliac Artery Compression Syndrome	302
5.5.1 2d Image	306
5.5.2 Colour Doppler	306
5.5.3 Spectral Doppler	306
5.5.4 Therapy	308
References	308
6 Doppler Sonography of the Liver in Infants and Children	311
6.1 Introduction	312
6.2 Technique and Investigation Standards	312
6.2.1 Different Doppler Techniques	312
6.2.2 Measurements and Indices	313
6.2.3 Important Parameters to Be Adjusted	315
6.2.4 Practical Considerations	315
6.3 Normal Findings	319
6.3.1 Basic Considerations	319
6.3.2 Liver Anatomy and Segment Classification According to Couinaud	321

6.3.3	Portal Vein	323
6.3.4	Hepatic Artery	327
6.3.5	Liver Veins	329
6.3.6	Normal Values	331
6.4	Doppler Sonography in Portal Hypertension	336
6.4.1	Basic Considerations	336
6.4.2	Prehepatic (Pre-sinusoidal) Block	340
6.4.3	Intrahepatic Block (Intra-sinusoidal PH)	341
6.4.4	Posthepatic Block	343
6.4.5	Other Causes for Portal Hypertension (PH)	345
6.4.6	Doppler Sonography for Assessment of Portosystemic Shunts	345
6.5	Doppler Sonography in Focal Liver Lesions	347
6.5.1	Introduction	347
6.5.2	The Role of Contrast-Enhanced US (CEUS) in Hepatic Focal Liver Lesions	348
6.5.3	Benign Focal Liver Lesions	349
6.5.4	Malignant Focal Liver Lesions	357
6.6	Other Applications of Liver Doppler Sonography	361
6.6.1	Various	361
6.6.2	Abernethy Syndrome	363
6.6.3	Heterotaxy Syndrome	364
6.7	Doppler Sonography in Paediatric Liver Transplantation	365
6.7.1	Hepatic Artery Occlusion	369
6.7.2	Hepatic Artery Stenosis	372
6.7.3	Portal Vein Stenosis	372
6.7.4	Stenosis of the Inferior Vena Cava	374
	References	375
7	Doppler Sonography of the Spleen	379
7.1	Introduction	380
7.2	Normal Findings	380
7.2.1	Embryology and Vascular Anatomy of the Spleen	380
7.2.2	Ultrasonographic Approach	381
7.3	Splenic Trauma	382
7.4	Focal Lesions of the Spleen	389
7.4.1	Introduction	389
7.4.2	Benign Splenic Lesions	389
7.4.3	Malignant Manifestations in the Spleen	396
7.5	Vascular Pathologies	396
7.5.1	Splenic Aneurysms	396
7.5.2	Splenic Pseudoaneurysms	398
7.5.3	Splenic Infarction	399
7.5.4	Peliosis	400
7.5.5	Flow in the Splenic Vessels in Congestive Conditions	401

7.5.6	Flow in the Splenic Vessels in Portal Hypertension	401
7.5.7	Thrombosis of the Portal Venous System after Splenectomy	401
7.6	Splenic Involvement in Infectious Diseases	402
7.7	Congenital Splenic Alterations	407
7.7.1	Wandering Spleen	407
7.7.2	Accessory Spleens (Splenuculi)	409
7.7.3	Splenosis	411
7.7.4	Polysplenia	411
7.8	The Role of Contrast-Enhanced US (CEUS) in Splenic Lesions	411
	References	412
8	Doppler Sonography of the Pancreas	415
8.1	Introduction	415
8.2	Normal Findings	416
8.2.1	Embryology of the Pancreas and Inborn Anomalies.	416
8.2.2	Pancreatic Vascular Anatomy	417
8.2.3	Ultrasonographic Approach	417
8.3	Doppler Sonography in Pancreatitis and Diffuse Lesions.	420
8.3.1	Introduction.	420
8.3.2	Acute, Chronic and Idiopathic Fibrosing Pancreatitis	421
8.4	Benign Focal Lesions of the Pancreas.	425
8.4.1	Cystic Lesions.	425
8.4.2	Solid Lesions.	425
8.5	Malignant Focal Lesions of the Pancreas	426
8.6	Pancreatic Trauma	427
8.7	Vascular Diseases	429
8.8	Doppler Sonography of the Pancreatic Graft	429
	References	430
9	Doppler Sonography of the Mesenteric Circulation	433
9.1	Introduction	434
9.2	Anatomy of the Splanchnic Circulation	434
9.3	Normal Values of the Flow Velocities in the Splanchnic Arteries	435
9.4	Dependency of the Flow Velocities on Age	435
9.5	Coeliac Artery	436
9.6	Superior Mesenteric Artery	436
9.7	Pathology	436
9.8	Intussusception	436
9.8.1	Reposition of the Intussusception.	441
9.8.2	Post-enema Sonography	441
9.9	Infectious Bowel Disease	442
9.9.1	Acute Inflammatory Bowel Disease	444
9.9.2	Chronic Inflammatory Bowel Disease	463

9.10	Vasculitis	468
9.11	Ischaemic Bowel Disease	469
9.12	Malrotation	470
9.13	Volvulus.	473
9.14	Strangulation	474
9.15	Hypertrophic Pyloric Stenosis.	474
9.16	Space-Occupying Lesions of the Gastrointestinal Tract	476
9.16.1	Cystic Gastrointestinal Lesions	476
9.16.2	Solid Gastrointestinal Lesions	479
9.16.3	Benign Lesions	479
9.16.4	Malignant Lesions	481
9.16.5	Lymphomas of the Gastrointestinal Tract.	481
9.16.6	Gastrointestinal Stroma Tumours.	482
9.16.7	Carcinoid Tumours.	483
	References.	485
10	Renal Circulation	489
10.1	Method.	490
10.2	Patient Preparation.	490
10.3	Technique.	491
10.4	Doppler Sonographic Flow Measurements in Renal Arteries Normal Values.	493
10.4.1	Dependency of the Arterial Flow Velocities on the Location of the Sample Volume	496
10.4.2	Dependency of the Arterial Flow Velocities on Age.	497
10.4.3	Dependency of the Arterial Flow Velocities on Weight	497
10.4.4	Dependency of the Resistive Index on Age.	497
10.5	Doppler Sonographic Flow Measurements in the Renal Veins Normal Values.	501
10.5.1	Dependency of the Venous Flow Velocities on the Location of the Sample Volume	501
10.5.2	Dependency of the Venous Flow Velocities on the Age	501
10.6	Pathologic Indications	502
10.6.1	Haemodynamic and Cardiovascular Diseases.	502
10.6.2	Stenosis of the Renal Artery	505
10.6.3	Renal Venous Thrombosis	509
10.6.4	Acute Renal Failure	512
10.6.5	Ureteral Jet.	529
10.6.6	Vesicoureteral Reflux.	531
10.6.7	Other Diseases of the Urinary Bladder	533
10.6.8	Doppler Sonography in Acute Renal Colic	535
10.6.9	Nephrolithiasis/Urolithiasis.	536
10.6.10	Traumatic Injury of the Kidney.	536
10.6.11	Renal Cysts	538

10.6.12	Renal Tumours	542
10.6.13	Kidney Transplantation	553
	References	563
11	Adrenal Glands	567
11.1	Method	567
11.2	Normal Adrenal Gland	569
11.3	Pathologic Indications	570
11.3.1	Congenital Adrenal Hyperplasia	570
11.3.2	Space-Occupying Lesions of the Adrenal Gland	570
11.3.3	Adrenal Haemorrhage	571
11.3.4	Adrenal Cyst	573
11.3.5	Neuroblastoma	574
11.3.6	Phaeochromocytoma	582
	References	588
12	CDI of the Ovaries	591
12.1	Introduction (Investigation Technique and Normal Findings)	591
12.1.1	Vascular Supply	592
12.2	Clinical Indications of Paediatric Duplex Sonography of the Ovaries	592
12.2.1	Ovarian Torsion Versus Inflammation	593
12.2.2	Cystic Disease and Other Ovarian Masses	594
12.2.3	Suspected Inguinal Herniation	596
	References	596
13	Doppler Sonography of the Scrotum	597
13.1	Introduction	598
13.1.1	The Normal Scrotum	598
13.2	Arterial Perfusion	599
13.3	Venous Drainage	600
13.4	Technical Prerequisites	600
13.5	Sonographic Anatomy	602
13.5.1	Indications for Investigation	605
13.6	Testicular Torsion	606
13.6.1	Extravaginal Torsion (in Neonatology)	606
13.6.2	Intravaginal Torsion (in Older Children)	607
13.6.3	Pitfalls of Testicular Torsion	612
13.7	Torsion of the Appendix Testes and Epididymis	614
13.8	Epididymitis and Orchitis	618
13.9	Systemic Disease with Scrotal Involvement	621
13.9.1	Acute Idiopathic Scrotal Oedema	621
13.9.2	Henoch-Schönlein Purpura	624
13.10	Scrotal Masses	624
13.11	Cystic Scrotal Masses	625
13.11.1	Peritesticular Fluid Collections	625
13.11.2	Testicular Cysts	629
13.11.3	Epididymal Cysts and Spermatoceles	629

13.12	Testicular and Paratesticular Neoplasms	630
13.12.1	Primary Testicular Neoplasms	632
13.13	Germ Cell Tumours	633
13.13.1	Yolk Sac Tumour	636
13.13.2	Teratoma	636
13.13.3	Seminomas	637
13.14	Non-Germ Cell Tumours	637
13.14.1	Juvenile Granulosa Cell Tumour	637
13.14.2	Leydig Cell Tumour	637
13.14.3	Secondary Testicular Neoplasms in Leukaemia and Lymphoma	637
13.14.4	Extratesticular Scrotal Tumours	638
13.15	Tumour-Like Lesions: Testicular Adrenal Rest Tumours in Postpubertal Males with Congenital Adrenal Hyperplasia	639
13.16	Testicular Microlithiasis	640
13.17	Inguinal Hernia	641
13.18	Haematoceles	642
13.19	Post-op	643
13.20	Varicocele	644
13.21	Testicular Trauma	648
	References	650
14	Duplex Sonography of Paediatric Peripheral Vessels and Soft Tissue	655
14.1	Introduction (Investigation Technique and Normal Findings)	655
14.1.1	Normal Arterial Flow	656
14.1.2	Normal Venous Flow	657
14.1.3	Interpretation of the Colour Map	659
14.2	Clinical Indication of Peripheral Vessel and Soft Tissue CDI	660
14.2.1	Colour Doppler-Guided Vascular Access Techniques	660
14.2.2	Vascular Disease (Venous and Arterial Occlusion)	661
14.2.3	Vascular Malformations and Haemangiomas	662
14.2.4	Other Soft Tissue Tumours	672
	References	676
15	Cardiovascular Diseases Which Influence the Flow in the Body Arteries	679
15.1	Introduction	680
15.2	Congenital Heart Diseases with a Leakage of the Aortic 'Windkessel'	680
15.2.1	Patent Ductus Arteriosus (PDA)	681
15.2.2	Common Arterial Trunk (TAC)	688
15.2.3	Aortic Septum Defect (Aorticopulmonary Window)	693

15.2.4	Aortic Regurgitation	694
15.2.5	Aorto-cameral Tunnel	694
15.2.6	Aorticopulmonary Shunt	694
15.2.7	Patent Ductus Arteriosus in Combination with Other Cardiac Malformations	699
15.2.8	Fallot Tetralogy and Pulmonary Atresia with Ventricular Septal Defect (VSD)	699
15.2.9	Critical Pulmonary Stenosis and Pulmonary Atresia with Intact Ventricular Septum	699
15.2.10	Tricuspid Atresia	702
15.2.11	D-Transposition of the Great Arteries	702
15.3	Cardiovascular Diseases with Obstruction of the Left Heart and Aorta	707
15.3.1	Critical Aortic Stenosis	708
15.3.2	Hypoplastic Left Heart Syndrome (HLHS)	710
15.3.3	Coarctation of the Aorta (COA)	712
15.3.4	Subclavian Steal Phenomenon	718
15.4	Cardiac Malformations Which Do Not Influence the Blood Flow in Peripheral Arteries	722
	References	730
	Index	731

Physical and Technical Principles of Doppler Sonography

1

Heiko Dudwiesus

Contents

1.1	Doppler Effect	2
1.1.1	Summary.....	4
1.2	Continuous Wave Doppler Ultrasound Technique	7
1.3	Spectral Analysis	9
1.4	Angle Problem	11
1.5	Pulsed Doppler Devices	14
1.6	Duplex Systems	19
1.7	Colour-Coded Doppler Sonography	20
1.8	Triplex Mode	26
1.9	Setting the Colour Threshold	27
1.10	Movement Disturbances and Wall Filters	28
1.11	Adjusting the Gain	30
1.12	Power Doppler	30
1.13	3D Dopplers	31
1.14	Non-Doppler-Based Flow Recording	32
	References	34

Abstract

The frequency shift postulated in 1842 by Christian Doppler as a consequence of a relative movement between wave transmitters and receivers was only utilized for the first time to capture intra-corporeal movements in the middle of the 20th century. During these initial experiments, Satomura first used an ultrasound beam focused on the heart to measure the contractile movements of the myocardium and later demonstrated that this method can also be used to detect blood flow.

When exposed to ultrasound, the frequency reflected by the corpuscular blood components changes as the reflectors approach the probe or move away from it. Since this frequency shift is proportionate to the flow velocity, by comparing the transmission and reception frequency, the velocity can be determined and displayed in the form of a spectral curve.

In CW (Continuous Wave) mode, all flows within the beam are captured, while PW (Pulsed Wave) mode allows the selective detection of flows along a narrowly circumscribed space known as the sample volume. To be able to visualize this sample volume, PW Dopplers are generally combined with imaging ultrasound equipment to create “duplex systems” and the measuring window displayed in the form of a cursor in the B image.

The color-coded Doppler creates a number of tiny measuring locations and selectively displays the documented flows in the form of corresponding pixels on a screen. The color

H. Dudwiesus
GE Healthcare GmbH,
Beethovenstr. 239,
42655 Solingen, Germany
e-mail: heiko.dudwiesus@med.ge.com

(usually red and blue) allows conclusions to be drawn about the direction of flow, while the flow velocity is expressed by the brightness of the corresponding pixels.

Echo signals that do not have their frequency shifted are evaluated as reflections of static structures and are displayed in the form of gray values. As a result, the color-coded (Color Flow) mode corresponds to a B-image with the location-correct display of flow information.

The Doppler ultrasound capture of flows is to a large degree dependent on the angle between the ultrasound beam and the flow axis, can sometimes fail when capturing very high velocities and demonstrates only limited spatial resolution. Additional alternative methods have also recently become available that are based on subtraction methods and which go some way towards overcoming the described shortcomings.

1.1 Doppler Effect

When Christian Doppler first presented his famous work *Über das farbige Licht der Doppelsterne und einiger anderer Gestirne des Himmels* (*On the coloured light of binary stars and some other stars of the heavens*) (Doppler 1842), the sceptical experts of the time were confronted with an unexpected thesis: The frequency which arrives at a receiver does not necessarily have to be the same as the one actually produced by the source. Doppler's hypothesis was a first attempt to explain the cause of the puzzling colour fluctuations of heavenly bodies circling one another. Inspired by references to the wave-form nature of light published previously, Doppler recognised the relative nature of the wavelengths detected and postulated that movements of either the wave generator or the observer changing the distance between them produce shifts in the frequency. Although Doppler's explanation for the cause of the colour fluctuations later turned out to be a misinterpretation, the basic idea of his thesis for the connection between movement and frequency detected proved to be an ingenious discovery. However,

Doppler was not able to prove that his hypothesis was correct at first. It was someone else's work (Buys-Ballot 1845; Mach 1873), which showed that the equation suggested by Doppler for calculating the frequency shift was actually correct. In this connection, the proportional relationship between the velocity and resulting shift in frequency proved to be extremely important – it enabled the velocity to be determined accurately and simply by comparing the source frequency with the frequency received.

Technical developments from the middle of the twentieth century showed that it was also possible to determine the speed of objects which did not actively generate a frequency. Accurate measurements could also be made by introducing energy from outside and using the reflected frequency.

Even now, the method of choice for determining the speed of an object, gas or other fluid in scientific or applied technology applications is still the Doppler technique for detecting movements. The Doppler effect is also still used to quantify blood flow velocities. Although new techniques (e.g. B-flow) which can detect and image the corpuscular blood components directly without using the Doppler effect produce a significantly more highly resolved and highly realistic image of the spatial blood vessel path and blood flow, they cannot be used to quantify the speed.

As everybody knows, it is the Doppler effect on sound waves which is used to detect arterial or venal flows because they show particularly large frequency shifts due to their relatively low propagation rate, are regarded as non-invasive according to current understanding and are reflected by the corpuscular blood components in the required manner.

The three image sequences in Fig. 1.1 show the frequency shift produced by the Doppler effect. The left sequence is an example of sound radiation at 1,000 Hz with the sound generator in a fixed position. During each millisecond, the oscillator exerts a short positive pressure pulse on the environment followed by a negative pressure pulse of equal duration caused by the oscillator snapping back. These pressure changes are also called acoustic waves and propagate into the surrounding medium at a speed determined by the nature of the medium. The length of the acoustic wave is determined by the frequency of oscillation.

tion and the propagation rate in the medium – the wavelength of sound at 1,000 Hz described here, for example, is 34 cm long in air.

The middle sequence of Fig. 1.1 shows a sound generator operating at the same frequency but moving to the right at a uniform speed of 100 m/s. At the beginning of the sequence, the sound generator is on the left and produces the sound pressure zone designated '1'. After 1 ms, this part of the sound wave is propagated 34 cm to the right due to the speed determined by the medium. However, the sound generator has also moved by 10 cm and is now already starting to emit the next pressure wave. In comparison to the stationary sound source, this second sound pressure zone has been displaced by 10 cm to the right so the spatial distance between the two pressure zones which have been produced one after the other (i.e. the wavelength) is of course shortened.

The consequence of this reduced distance is that the pressure maxima arrive at the receiver with shorter time intervals so the receiver receives more pressure zones per second than would have been the case had the sound source remained sta-

tionary. The perceived frequency is therefore higher than the frequency actually produced.

In the example described here, the sound frequency received would be 1,416 Hz instead of 1,000 Hz which was the frequency at which the sound was generated. As Doppler correctly postulated, the displacement speed of the sound source is proportional to the change in frequency.

If, on the other hand, the sound source moves away from a receiver, the distance between two sound pressure zones will increase (Fig. 1.1 right). In this example also, the sound pressure zone designated '1' is emitted first and has moved about 34 cm to the right 1 ms later, due to the speed of sound in air. At the same time, the sound source has moved around 10 cm to the left and started to emit the next pressure zone from this point. The distance of 34 cm between the two pressure waves has therefore lengthened to 44 cm. A receiver would therefore receive the pressure waves with longer time intervals and would therefore register a lower frequency of just 773 Hz.

Changing the location of a sound source, however, is not the only way a frequency shift may be

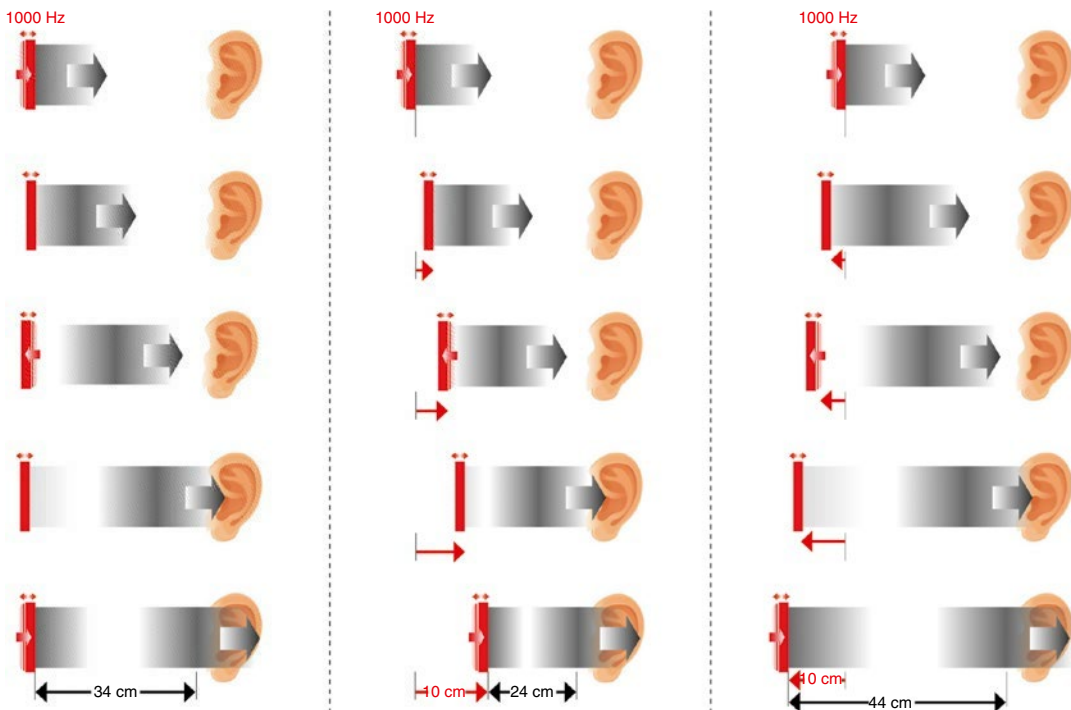


Fig. 1.1 (Left) Generation and propagation of sound waves. (Centre) Shortening of sound waves caused by an approaching acoustic source. (Right) Prolongation of sound waves when the acoustic source is moving away

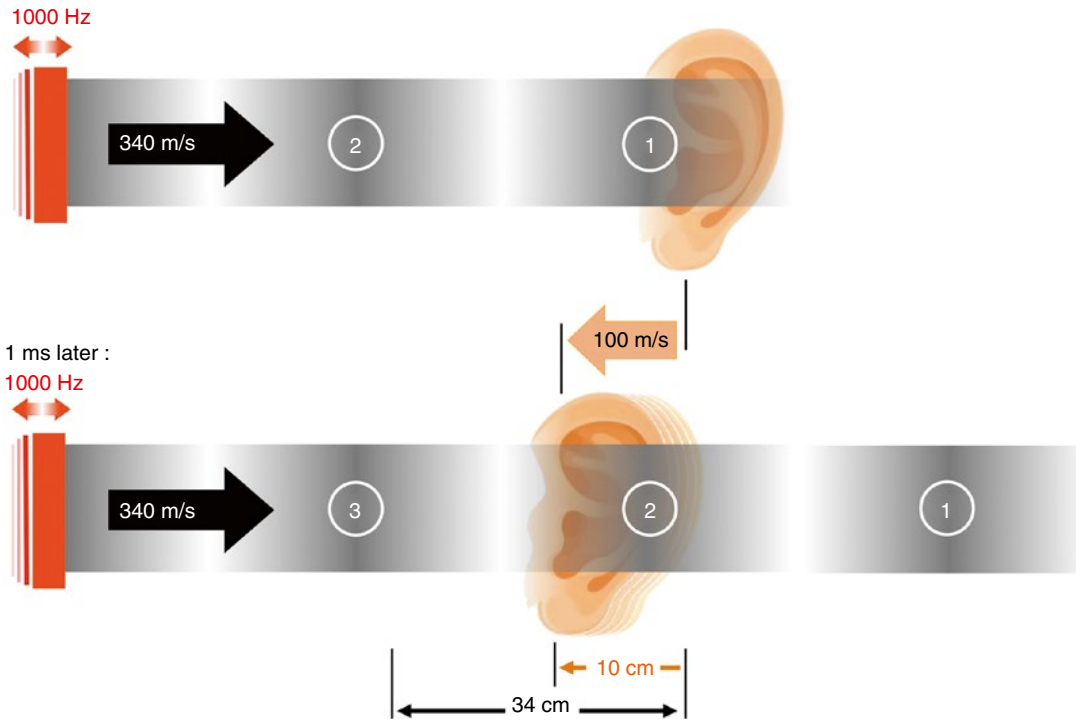


Fig. 1.2 Increase of observed frequency when the receiver is moving towards

produced – a corresponding effect is also experienced by moving the receiver.

This phenomenon is illustrated in Fig. 1.2.

The receiver in the figure moves at a speed of 100 m/s towards the approaching sound waves. The top of the figure shows that the pressure maximum designated '1' arrives at the observer. The high pressure zone designated '2' follows at a distance of 34 cm (in accordance with a sonic frequency of 1,000 Hz) and would normally reach the observer 1 ms later. Since the latter has moved closer to the sound generator by around 10 cm, the sound wave '2' arrives correspondingly earlier – i.e. after less than a millisecond. The shortening of this interval corresponds to an increase in the perceived frequency from 1,000 to 1,294 Hz.

On the other hand, if the observer moves away from the transmitter, the number of sound waves detected per second decreases. This is clearly shown in Fig. 1.3. At the top of the figure, the observer hurrying away receives the sound wave designated '1' at a frequency of 1,000 Hz. The wave designated '2' generated after a millisecond

has to travel a longer distance than sound wave '1', since the observer has now moved 10 cm further away from the sound source. In this case, the interval between two reception cycles thus increased corresponds to a reduction in frequency from 1,000 to 706 Hz.

If the departure velocity were to increase to the speed of sound, the observer would find himself moving forwards with the sound wave inside a constant pressure zone. In this extreme case, periodic pressure changes would cease to arrive at the receiver and the frequency detected would be zero.

1.1.1 Summary

- Transmitter approaches receiver = increase in perceived frequency
- Transmitter moves away from receiver = decrease in perceived frequency
- Receiver approaches transmitter = increase in perceived frequency

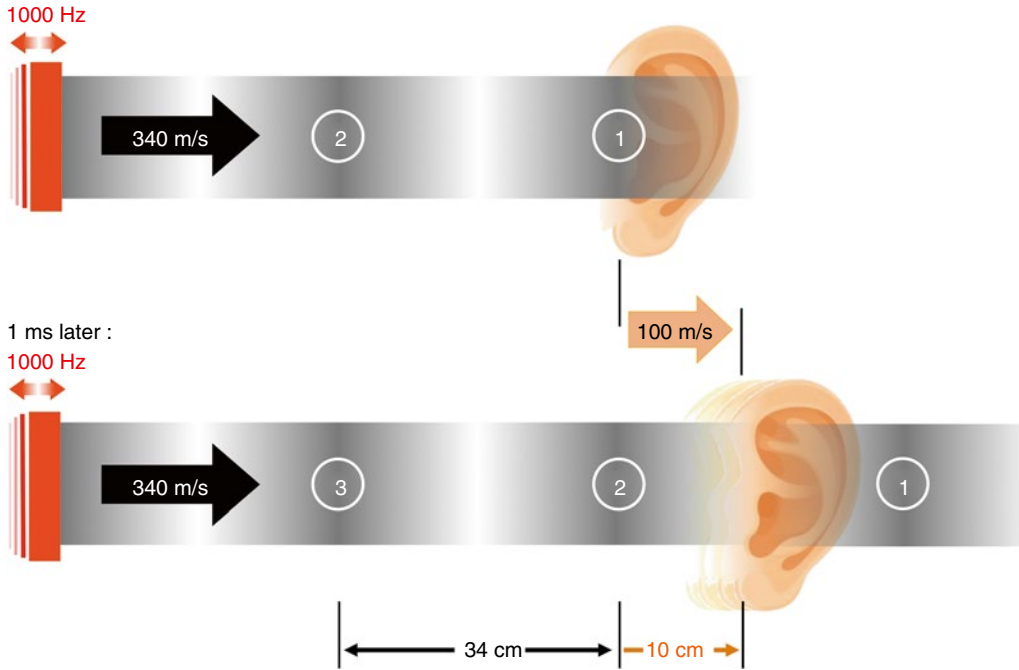


Fig. 1.3 Decrease of observed frequency when the receiver is moving away

- Receiver moves away from transmitter = decrease in perceived frequency

Since the situation is different in each case, Christian Doppler derived a different equation to calculate the frequency shift depending on whether the sound source or the observer is moving. However, if the speed of the object is small in relation to the speed of sound, the same

simplified calculation principles can be applied to both cases. Thus, the frequency shift has one proportionality ratio both for the original frequency produced by the sound generator and for the speed of the observer or the sound source. On the other hand, the frequency shift is inversely proportional to the speed of sound in the medium. The simplified equation is therefore:

$$\text{Frequency shift } f_d \text{ (Hz)} = \frac{\text{Original frequency } f_o \text{ (Hz)} \times \text{Speed } V \text{ (m/s)}}{\text{Speed of sound } C \text{ (m/s)}}$$

The Doppler effect is certainly experienced in everyday life. For example, an observer will notice a change in pitch of the sound coming from a fast car as it passes the point of observation on a fast road. As the car approaches, the observer hears a sound which is higher pitched

than the sound of the engine. Once the vehicle has reached the hearer and is moving away, the sound waves are ‘stretched’ and the observer hears the sound at a lower pitch.

The frequency also changes when the distance between the sound source and sound receiver does

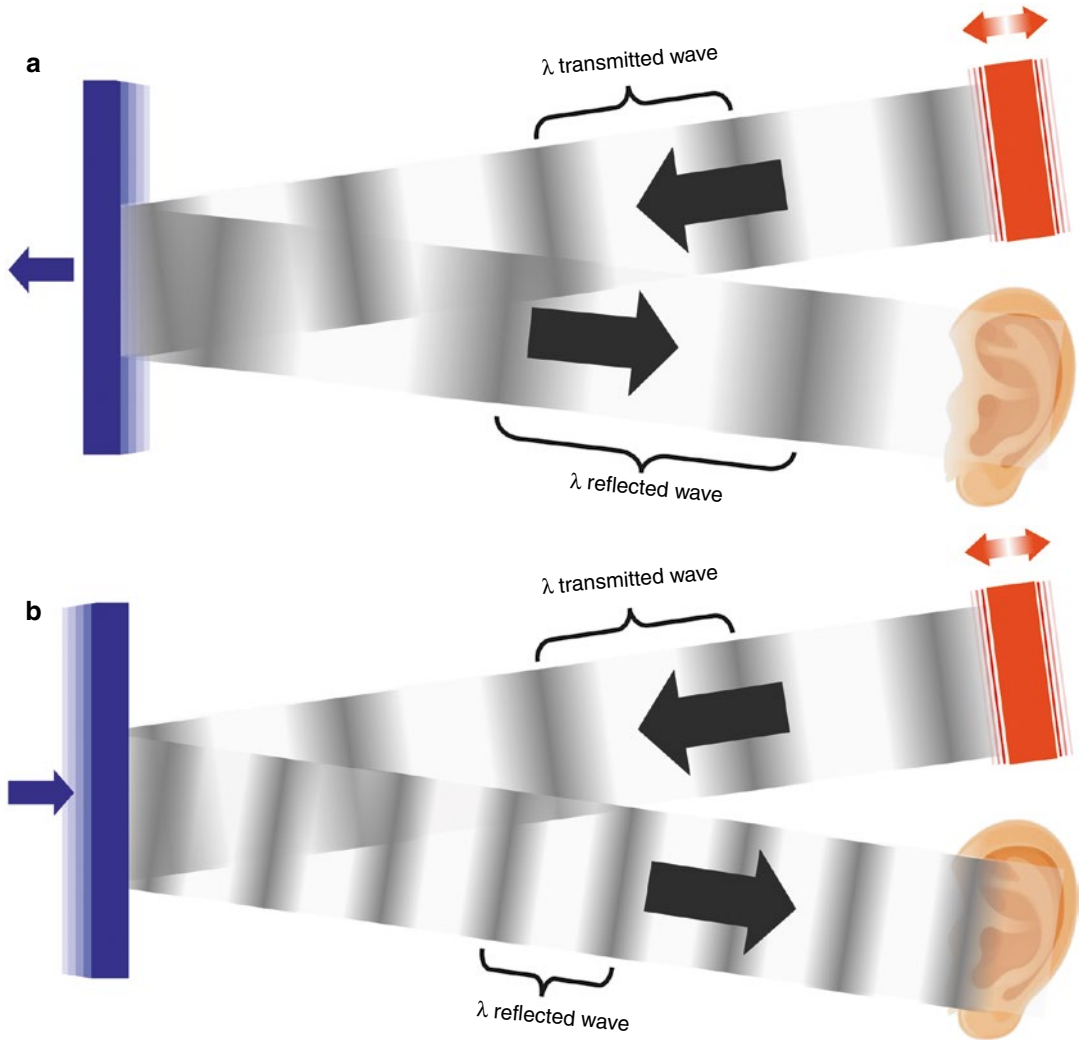


Fig. 1.4 (a, b) Change of the observed frequency when the reflector is moving away or towards

not change but the sound is deflected via a moving reflector (Fig. 1.4). Since the first Doppler shift has already taken place on arrival at the reflector and the second Doppler shift takes place when it

is emitted at a frequency which has already changed, the frequency change is doubled.

In this case, the Doppler equation must be modified as follows:

$$\text{Frequency shift } f_d (\text{Hz}) = \frac{\text{Original frequency } f_0 (\text{Hz}) \text{ Speed } V (\text{m/s}) \times 2}{\text{Speed of sound } C (\text{m/s})}$$

If the original frequency is known and the reflected frequency is measured, the speed of the reflector can also be measured by rearranging the equation. This principle is used in research, medicine and industry as well as the police force,

military applications and by aerospace authorities to determine the approach speed of vehicles, aircraft or rockets. In these cases, the object being checked is not subjected to sound waves but high-intensity long-range electromagnetic waves.

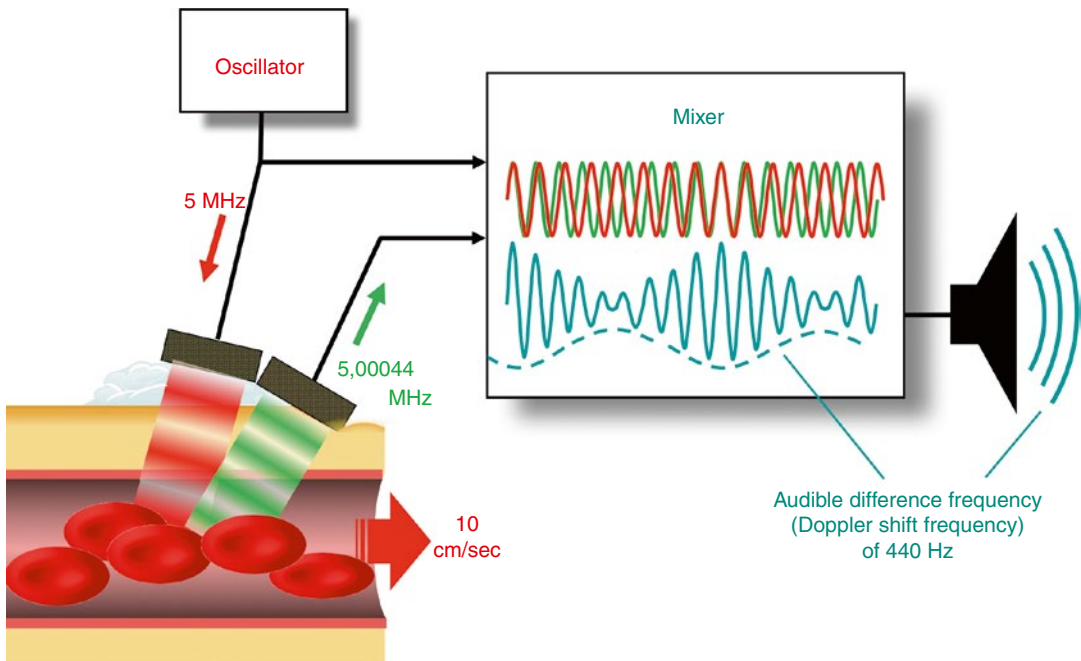


Fig. 1.5 Functional principle of a simple CW-Doppler without display

Different methods are available for Doppler sonographic flow measurements in medicine which will be dealt with in more detail in the following – the continuous wave Doppler, the pulsed wave Doppler and the different colour-coded Doppler techniques.

1.2 Continuous Wave Doppler Ultrasound Technique

The principle of frequency shifts caused by a moving reflector described above is used to measure blood flow velocity (Satomura 1959; Strandness et al. 1967).

Ultrasound is continuously radiated into the body at a frequency between 2 and 10 MHz from a quartz crystal (Fig. 1.5). Minute components of the energy are reflected back by the tissue, vessel walls and even the surfaces of the corpuscular blood components and picked up by a second crystal. The detected ultrasound is fed to a so-called mixer where it is compared with the transmission frequency. Since there is no difference between the frequencies of the sound reflected back from the static reflecting surfaces to the fre-

quency of the transmitted sound, the mixer will not detect any difference between them.

The moving blood cells, however, reflect back the radiated sound at a different frequency according to the Doppler principle. The greater the rate of flow, the greater the difference between the frequency of the reflected sound and the frequency of the radiated sound. With a transmission frequency of 5 MHz and a velocity of 10 cm/s, the ultrasound frequency shifts from 5,00,000 to 5,00,044 MHz. To determine the difference, the transmitted and received frequencies are superimposed so that they alternate between coincidence and noncoincidence as a result of the slight difference in wavelengths. At the same time, the amplitude is always increased by addition when both signals are exactly in phase, i.e. have the same polarity. On the other hand, if the ultrasound frequency has a positive amplitude while the other signal is negative, the net result is extinction. This produces a new frequency which corresponds exactly to the difference between the transmitted ultrasound frequency and the received ultrasound frequency. In the example here, the difference is 440 Hz, which can be heard as a howl or a hiss in the loudspeaker.

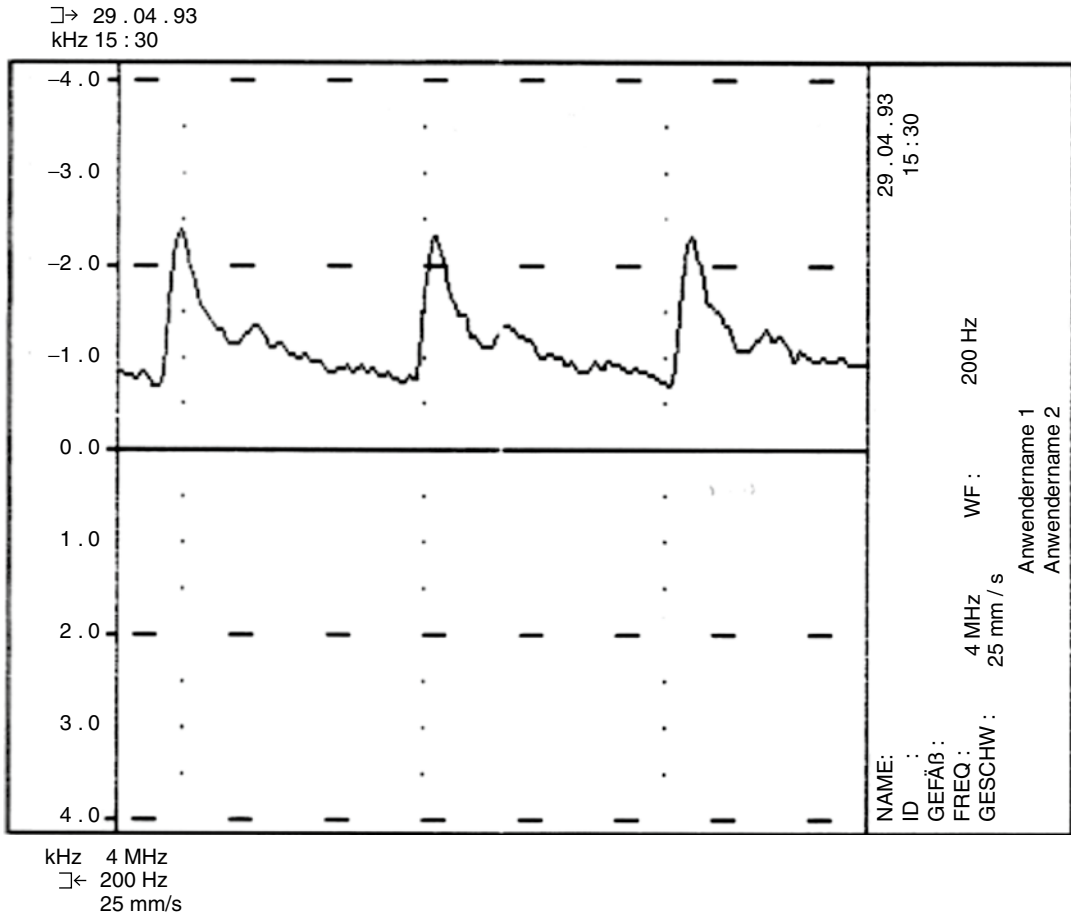


Fig. 1.6 Print out of a Doppler curve by application of a zero crosser signal processing

The faster the blood velocity, the greater the difference between the transmitted frequency and the received frequency and the greater the perceived difference or Doppler frequency

Since blood flows at an almost uniform rate in the veins, the noise coming from the device during a venal examination is an almost constant howl. On the other hand, the flow pulsation in the arteries causes the sound pitch to swell and subside as the Doppler frequency changes with the cardiac cycle.

Although this simplest of all Doppler devices only provides acoustic information about flow behaviours, it can be used for numerous applications in angiological diagnostics (Marshall 1984; Fischer and Wuppermann 1985; Mühlen 1989).

Since the acoustic signal from this device corresponds merely to the difference between the transmitted and received frequency, it is possible to draw conclusions on the flow velocity only – not on the flow direction. Both a blood flow towards the probe and a blood flow away from it but of identical flow velocity will produce an identical frequency shift. This technique is therefore called ‘*non-directional*’.

The Doppler systems which indicate the direction of flow have a wider range of applications. The signal processing system of these devices is able to detect the direction of flow in relation to the probe and display it as a velocity curve on the screen or printer (Fig. 1.6). Usually, these *directional Dopplers* are polarised so that flows towards the probe are displayed above and flows away from the probe are displayed below the zero line on the screen. However, this arrangement can be inverted

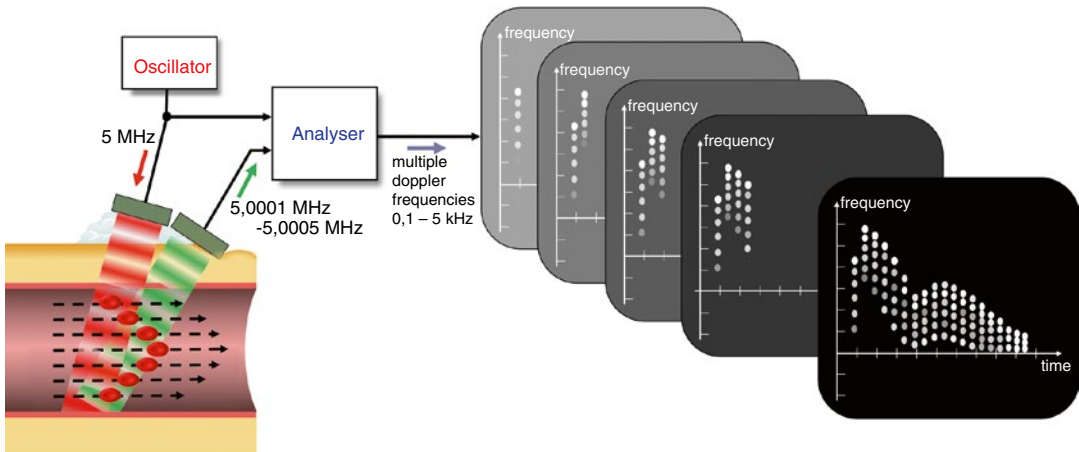


Fig. 1.7 Acquisition and display of a Doppler frequency spectrum

on every commercially available device. The size of the deflection, i.e. the amplitude of the curve, reflects the flow velocity under examination.

Simple devices use a so-called *zero crosser* to convert the Doppler frequency into a proportional deflection. Here, the frequency of the Doppler signal is simply ‘counted out’ and converted into an analogue deflection (MacLeod 1967).

These devices therefore do not take into account the fact that the corpuscular blood components move at very different rates over the cross section of the vessel. Since the zero crosser is not able to record several speeds simultaneously, only the predominant speed (i.e. the speed at which the overwhelming majority of particles are moving within the observation time) appears on the screen. All other speeds are disregarded (Lunt 1975; Evans et al. 1989).

However, since the evaluation during Doppler sonographic examinations predominantly relies on measuring the peak velocity (Gosling 1971; Gosling and King 1974; Planiol and Pourcelot 1973), applying zero crossing is out of the question for all quantitative and semi-quantitative analyses.

1.3 Spectral Analysis

In contrast to the zero-crossing technique, spectral analysis shows all the speeds over the cross section of the vessel (Maulik 2005). In addition to this, the frequencies or velocities on the screen are correct,

so it is possible to make quantitative statements by including other measurement parameters (Warnking and Teague 1981). In principle, the velocity spectrum displayed on the screen or printer corresponds to the conventional Doppler curves with a vertical speed axis and horizontal time axis.

Figure 1.7 shows how it operates schematically. In order to show all the speeds simultaneously, the particle speeds detected are displayed on the vertical axis in the form of dots one on top of the other. Each dot therefore corresponds to a certain frequency or speed. Each speed causes its own Doppler shift so the receiving crystal detects a variety of different ultrasonic frequencies. However, since this receiving crystal cannot oscillate at all the frequencies simultaneously, they are superimposed additively to produce a new, quite complex curve shape. Inside the spectrum analyser, this frequency mix is compared with the original transmitter frequency to produce numerous different Doppler or difference frequencies. Thus, the slow velocity at the wall yields a Doppler frequency of a few Hz, while the highest speed which is often in the centre of the vessel can produce a frequency shift of up to 10 kHz or more, for example.

These Doppler frequencies are displayed on a vertical frequency axis on a screen in the form of pixels. Each dot therefore represents a certain frequency or speed. The intensity of each dot represents the occurrence of the corresponding speed. Thus, dots which are particularly intense indicate that there are a lot of blood cells moving at this speed.

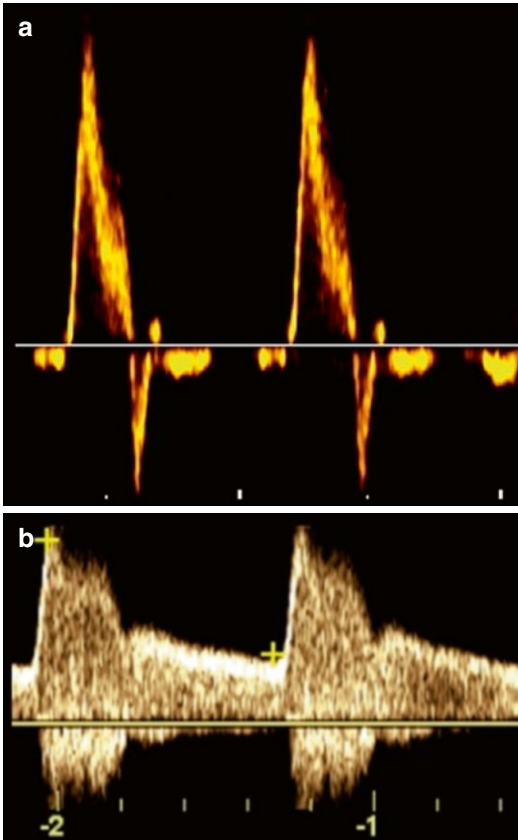


Fig. 1.8 (a) Frequency spectrum of an undisturbed laminar flow. (b) Frequency spectrum of a turbulent flow

The frequency analysis and the structure of the corresponding vertical dot line are completed after a few milliseconds. A new measurement cycle then starts immediately where the frequencies which are now determined are displayed to the right of the previous line. Thus, the picture develops line-by-line in quick succession as the speed curve is displayed to the observer and scrolls across the screen in real time.

Under normal conditions, the blood flow is predominantly laminar, i.e. the corpuscular blood components flow in a straight or – as we now know – in a helical (Kilner et al. 1993) way on parallel paths. In this case, the flow rate profile is plug shaped, i.e. most particles move at approximately the same speed – only the particles in the direct vicinity of the wall move at a lower speed due to friction. As shown in Fig. 1.8a, the spectrum analyser in this case dis-

plays a narrow-band frequency curve. Low speeds are underrepresented, particularly during the systolic phase, and the so-called systolic window appears, i.e. an almost dot-free area below the ends of the curve envelope. The dots representing the higher speeds are particularly intense on the display.

Sometimes, particularly when higher speeds are displayed on the screen due to stenosis, the laminar nature of the blood flow can be substantially disrupted. In this case, the particles no longer move along straight parallel paths but change their paths and speeds; sometimes, eddies and other disturbances occur. Since this type of turbulent flow produces many different speeds simultaneously, the Doppler spectrum appears as a broad band during the systolic phase, and the curve between the zero line and the peak value is relatively uniformly filled with dots (Fell et al. 1981) (Fig. 1.8b). Components of the flow moving in opposite directions as they occur inside the eddies appear below the zero line on the Doppler spectrum.

Since the amplitude of the curve on the spectrum is exactly proportional to the actual peak velocity, this method makes it possible to carry out at least semi-quantitative evaluations, in order to calculate and use indexes, for example. The Resistance Index according to Pourcelot (Planiol and Pourcelot 1973) has proved particularly effective for most applications. This index makes it possible to draw conclusions about the perfusion resistance downstream of the measurement site by comparing the height of the systolic peak flow velocity with the end-diastolic peak flow velocity. The equation is as follows:

$$RI = \frac{S - D}{S}$$

where ‘S’ is the systolic peak frequency and ‘D’ is the highest end-diastolic frequency.

Figure 1.9a shows typical flow-velocity curves as a function of the subsequent perfusion resistance and the RI calculation. A low peripheral resistance is accompanied by a high diastolic amplitude and low RI. On the other hand, a high peripheral resistance is characterised by low diastolic amplitude and a high RI (Fig. 1.9b).

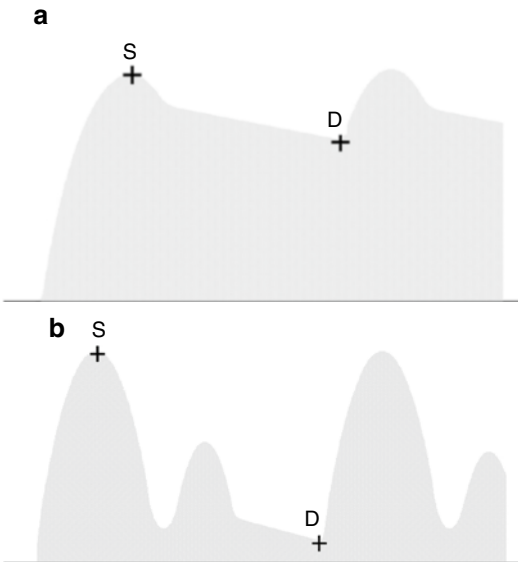


Fig. 1.9 (a) Schematic flow curve of a vessel supplying an area with low perfusion resistance. (b) Schematic flow curve of a vessel supplying an area with high perfusion resistance

Modern Doppler systems can detect the relevant measurement points S and D automatically and display the index on the screen in real time.

One alternative to the Resistance Index is the somewhat more complex Pulsatility Index of Gosling (Gosling and King 1974; Gosling et al. 1971). In contrast to the RI, this index not only detects the systolic and the end-diastolic peak but also takes into account the entire curve for the cardiac cycle, including any retrograde flow components which may be present. The peak-to-peak frequency must also be determined, i.e. the difference between the maximum and minimum frequency, where the minimum may also lie below the zero line in the case of an early diastolic retrograde dip (Fig. 1.10). Furthermore, an average value for the envelope must be calculated over one cardiac cycle – and this requires an electronic calculation.

The Pulsatility Index is produced from the ratio of the peak-to-peak value to the average value.

$$PI = \frac{\text{Peak-to-peak frequency}}{\text{Time-averaged maximum frequency}}$$

Note: Some ultrasound systems offer different algorithms for determining the average value, e.g. by recording the integral, i.e. of all the frequencies beneath the envelope curve (TAM – time-averaged mean frequency). The PI values determined using these algorithms do not correspond to the measurement results based on the envelope curves. This must be taken into consideration during the evaluation and when comparing with the standard values.

1.4 Angle Problem

As already explained above and shown by the Doppler equation, a proportional relationship exists between the blood velocity and the Doppler frequency or the curve amplitude on the screen. However, this proportionality does not allow the determined Doppler frequency to be converted directly into the absolute blood velocity in m/s or cm/s.

This is due to the strong dependence of the Doppler frequency on the angle between the ultrasound beam and the direction in which the reflectors move. It is not the absolute speed of a reflector which is crucial for the development and intensity of the Doppler effect, but the velocity at which the distance between the reflector and the Doppler scan head changes. The difference between the absolute and detected velocity is illustrated in Fig. 1.11. While the erythrocyte moves at 1 cm per second in relation to its environment, its change in distance to the Doppler probe is smaller. For example, if the initial distance is 10 cm, the final distance after 1 s is only reduced to 9.3 cm. Therefore, from the point of view of the Doppler scan head, the approach velocity of the erythrocyte is merely 0.7 cm/s which means that the measured velocity is 30 % less than the actual velocity.

The angle between the direction of movement and the direction of observation is crucial for the difference between the measured velocity and the actual velocity – the wider the angle, the greater

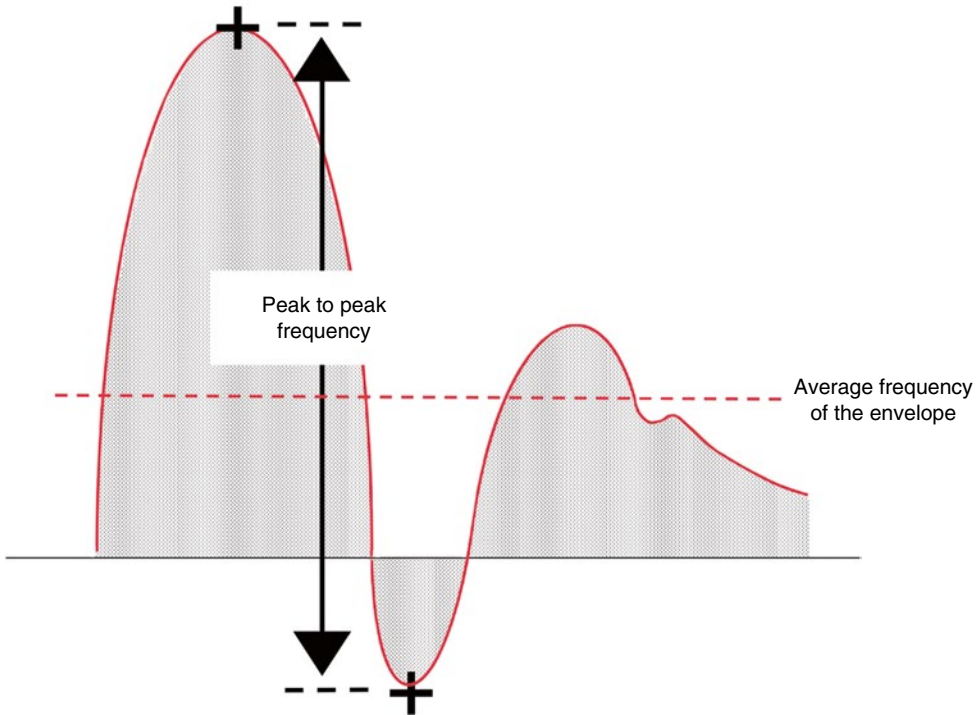


Fig. 1.10 Measuring points for calculation of the pulsatility index

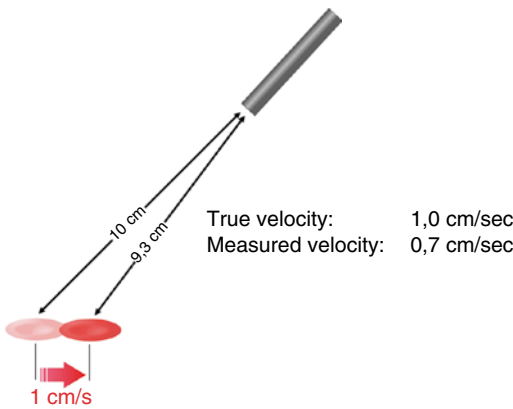


Fig. 1.11 Difference between true velocity and approach velocity

the discrepancy between the actual forward movement and the measured approach velocity (Fig. 1.12).

With angles up to approximately 20° , the discrepancy is small and the detected Doppler frequency only deviates a little from the value which would be attained under the ideal conditions of 0° .

The deviation is calculated very easily from the cosine of the angle. At 0° (when the erythrocytes move directly towards or away from the probe), the cosine=1 so that the genuine frequency shift occurs according to Doppler's equation. At an angle of 15° , the cosine decreases to 0.97. Since this value enters the Doppler equation as a multiplication factor, the Doppler frequency which occurs drops to 97 % of the original value. The corresponding measurement error of 3 % can of course be disregarded. Even at 30° and a corresponding cosine of 0.87, the deviation amounts to a tolerable 13 % and is therefore still within the usual biological scatter of Doppler sonographic standard values. At 45° , the error increases to 25 % and at 60° , to a significant 50 % rising quickly as the angle widens. At 75° , the cosine is only 0.26 and the Doppler frequency detected by the equipment is therefore only 26 % of the frequency which would be produced under the optimum angle conditions. As the angle increases further to 90° , the cosine finally decreases to the value '0', so the Doppler frequency detected is only 0 % of the optimum

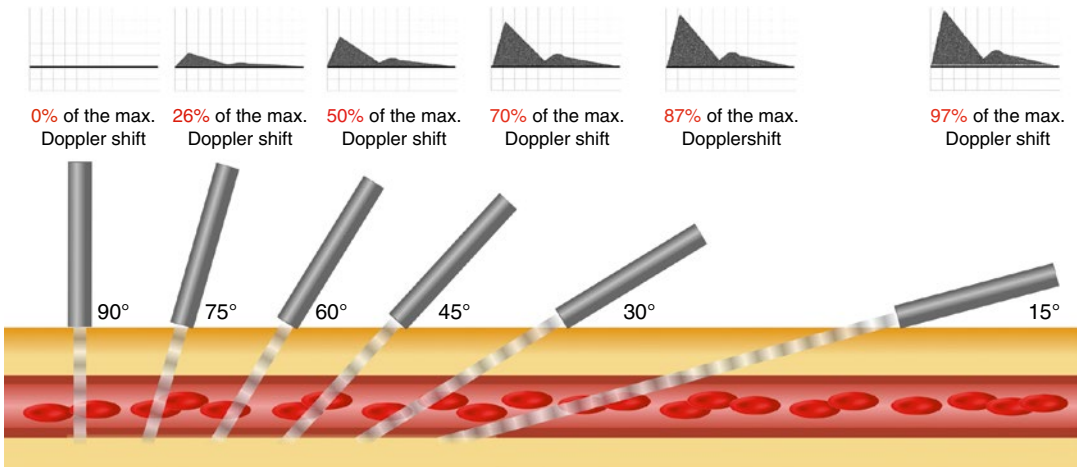


Fig. 1.12 Angle dependency of the Doppler frequency

value. The erythrocytes pass under the ultrasonic beam at right angles so they neither approach nor move away from the probe and no longer give rise to a Doppler effect. The spectral display on the screen usually only shows weak interference signals in the region of the zero line, and the Doppler signals which are heard are mainly caused by movements of the vessel wall.

As the matters discussed previously show, the examining physician should always endeavour to obtain an acute-angled beam of the target vessel and place the probe accordingly in order to produce the optimum signal. Experts largely agree that angles wider than 60° cannot be relied on to produce a sufficiently large Doppler shift and the frequency spectra they produce should not be assessed. If the angle which can be obtained is between 30° and 60° due to the anatomical condi-

tions, the question how to continue the procedure depends on the objective of the examination and must be determined by the following criteria:

- With a purely qualitative evaluation of the frequency spectrum, particularly when the Resistance or the Pulsatility Index is used for the evaluation, the differences in frequency caused by the angle are immaterial since the systolic peak frequency is falsified to the same degree as the diastolic peak. The frequency spectrum displayed can therefore be used for the evaluation without further measures.
- On the other hand, if the aim is to acquire a quantitative measurement of the flow velocity, the angle between the ultrasonic beam and the axis of flow must be known so that the cosine of this angle can be used for conversion into m/s or cm/s.

$$\text{Flow velocity (m/s)} = \frac{\text{Doppler frequency (Hz)} \times \text{Speed of sound (m/s)}}{\text{Ultrasound frequency (Hz)} \times 2 \times \cos \theta}$$

Because Doppler and B-mode imaging sonography are normally used in combination today, the angle can be seen directly on the screen by manually adjusting the angle cursor along the direction of flow visualised by the B-mode sonography. The system computer therefore receives the necessary information about the angle between the

ultrasound beam and the axis of flow, determines the cosine automatically and takes this value into account when outputting the data and scaling the Doppler curve (see also the Sect. 1.6, Fig. 1.20).

If it is possible to use an acute angle of 30° or even narrower, there is usually no need for correction in the case of quantitative measurements

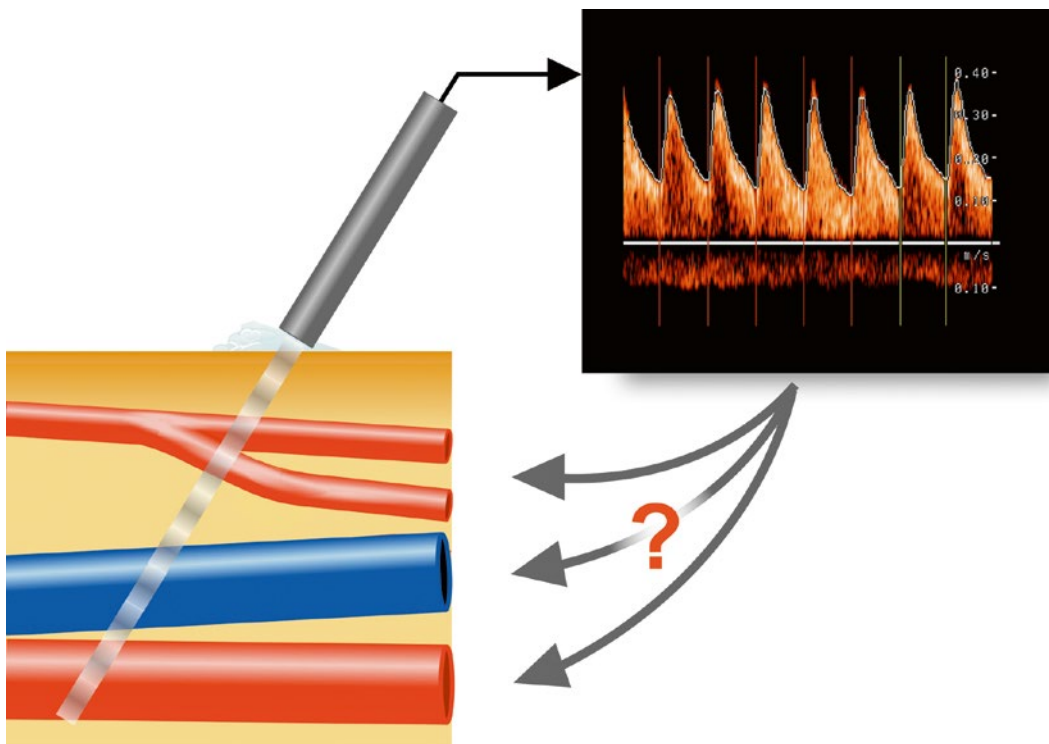


Fig. 1.13 Missing possibilities of depth selection by using CW Doppler

since the Doppler frequency detection error can be neglected (underestimation of 13 %).

1.5 Pulsed Doppler Devices

When there are other blood vessels between the Doppler probe and the vessel under examination, the *continuous wave technique* (CW Doppler) described above will not work because it is unable to target the depth. Continuous wave devices with their continuous sound transmission detect all the blood flows present within the range of the ultrasonic beam (Fig. 1.13).

With pulsed Doppler devices, however, blood vessels can be selected for measurement within a range of depths which can be chosen beforehand (Baker 1969).

Pulsed Doppler systems do not transmit continuous ultrasound but wave packets of short duration (bursts) lasting just a few microseconds each. Immediately after a transmission pulse has been transmitted (Fig. 1.14a), the crystal in the ultrasonic probe is switched to the receiver in order to detect the sound reflected back (Fig. 1.14b). However, not

all the reflected signals are processed, but only those which are reflected back at a certain time and, therefore, from a certain depth (Fig. 1.14c). Echoes which arrive too early, i.e. from close range, and signals which return very late, i.e. from greater depths, are ignored (Fig. 1.14d).

The time window and, therefore, the depth where the measurement is to take place can usually be varied using a suitable controller, 'blind' either by means of a device with a cm scale or by placing a cursor inside a reference ultrasonic image on the screen.

In most cases, the length of time the receiver is switched on can be changed so that the axial length of the measurement site can be varied. However, the lateral dimension depends on the diameter of the ultrasonic beam alone and cannot be varied with the latest technology. Since the volume examined represents a three-dimensional space, it is frequently also referred to as 'sample volume'.

Once the specified waiting period has elapsed and the expected echoes have been received, the crystal can be used again to send out the next transmission pulse. The frequency at which these transmission pulses are sent, the so-called *pulse*

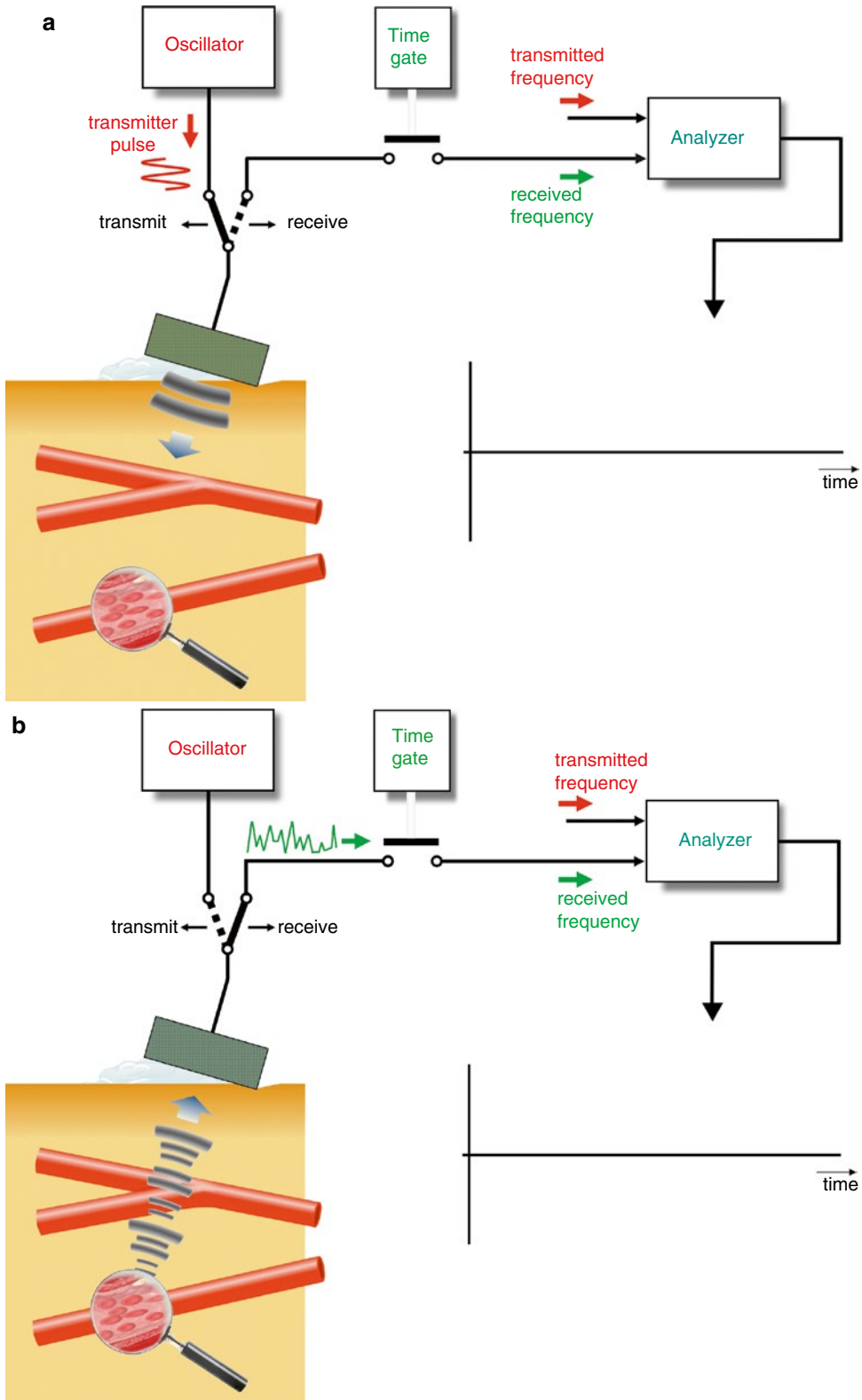


Fig. 1.14 Functional principle of the PW Doppler. (a) Transmission of the ultrasound burst. (b) Switch to reception whereas unwanted signals from the near field are ignored. (c) Time gate switches to admission, signals coming from the target area are processed. (d) Time gate switches to block, signals from greater depths are ignored